Effect of Free Polymer on the Structure of a Polymer Brush and Interaction between Two Polymer Brushes

C. M. Wijmans,† E. B. Zhulina,‡ and G. J. Fleer*

Department of Physical and Colloid Chemistry, Agricultural University Wageningen, Dreijenplein 6, 6703 HB Wageningen, The Netherlands

Received December 7, 1993; Revised Manuscript Received March 18, 1994®

ABSTRACT: Self-consistent-field (SCF) calculations are presented of a planar grafted polymer layer that interacts either with free polymer chains or with another grafted layer. Three different systems are studied. The first is a grafted polymer layer immersed in a polymer solution. The interaction between grafted and free polymer can significantly influence the grafted polymer volume fraction profile. For grafted chains that are strongly stretched the lattice calculations are compared with the theory of Zhulina, Borisov, and Brombacher (*Macromolecules* **1991**, *24*, 4679). Good agreement is found when the free chain length is far smaller than the grafted chain length. The scaling behavior of the penetration of free polymer into the grafted layer is also studied for this system. In the second type of system the interaction between two grafted layers in the absence of free polymer is considered. The lattice calculations agree well with the theory of Zhulina *et al.* In the third system free polymer is present between the interacting grafted layers. If this free polymer has a small chain length, its main effect on the interaction free energy is the compression of the free grafted layers, and only repulsion is found. However, for larger chain lengths a depletion attraction between the grafted layers appears.

1. Introduction

In a previous paper[1] the self-consistent-field (SCF) description of noncompressed polymer brushes was discussed. Assuming that the chains in such a brush are strongly stretched with respect to their free Gaussian dimension, one can elegantly describe the structure of such a system by following a suggestion first introduced by Semenov.[2] In this approach all possible conformations of the polymer chains are replaced by a set of the most probable conformations. For a given system this assumption can be rigorously checked using a SCF theory that involves the generation of all possible chain conformations on a lattice. The assumption of strong chain stretching is valid for a polymer brush immersed in a low molecular weight solvent under a very wide range of solvent strengths, but this assumption breaks down under extreme conditions, notably for very short grafted chain lengths. A polymer brush containing long grafted chains immersed in a solution of short mobile chains behaves in a way similar to that of a brush in pure solvent.

In this paper we shall discuss interactions between grafted layers in the absence and in the presence of free polymer. First, we discuss an isolated brush immersed in a solution of free polymer with the same chemical composition (but not necessarily the same degree of polymerization) as the grafted polymer. Here, the interesting issue is to what extent the free polymer penetrates into the grafted layer. Scaling dependencies will be derived for the degree of interpenetration as a function of grafting density, free and grafted chain lengths, and free polymer concentration. Second, the interaction between two planar grafted polymer layers immersed in a solvent will be considered. Milner *et al.*[3] and Zhulina *et al.*[4] showed how the strong chain-stretching description of a single polymer brush can be extended to describe the interaction between two grafted layers if the interpenetration of these two layers is neglected. By comparing the predictions of this theory with the results of lattice calculations, we hope to gain more insight into the behavior of compressed polymer layers. In particular the effects of weak chain stretching and the interpenetration of opposite layers will be studied. The third system discussed in this paper is a combination of the two previous ones: the interaction of two grafted layers in a solution of free polymer. In section 2 the theoretical methods are described, in section 3 numerical and analytical results are given, and in section 4 we discuss these results.

2. Theory

Lattice Model. Grafted polymer, solvent, and free mobile polymer are distributed on a planar lattice, consisting of M layers of L sites each, between two parallel plates. The diameter, l, of the segments defines the lattice spacing. We restrict ourselves to the case of grafted and free polymer molecules of identical segment types in an athermal solvent. For large interplate distances Ml this system reduces to that of two isolated polymer brushes immersed in a polymer solution. If Ml is smaller than twice the brush thickness, we have two brushes in interaction. We consider polymer chains that are grafted at one end onto one of the two plates with a relative surface coverage $\sigma = n_g/L$, where n_g is the total number of chains grafted to that plate. In general, we want to compute the equilibrium distribution of all three components on the lattice for given values of M, σ ($0 \le \sigma \le 1$), grafted chain length N_g, free chain length N_f, and bulk volume fraction ϕ_f^b of the mobile polymer ($0 \le \phi_f^b \le 1$). This is done by weighting all possible conformations of the polymer chains by their Boltzmann probability factor. In a previous paper[1] we showed how the Scheutjens–Fleer formalism for polymer adsorption can be used to find the volume fraction profiles of such systems with grafted chains in the presence or absence of free polymer. In that paper we also discussed the computational problems that arise when long polymer chains are considered with a high grafting density.

For two interacting brushes the free energy $A(M)$ of the system can be calculated as:[5]

† Present address: Physical Chemistry 1, Chemical Center, University of Lund, P.O. Box 124, S-221 00 Lund, Sweden.
‡ Permanent address: Institute of Macromolecular Compounds, Russian Academy of Science, St. Petersburg 199004, Russia.
® Abstract published in *Advance ACS Abstracts*, May 1, 1994.

0024-9297/94/2227-3238$04.50/0

$$\frac{A(M)}{LkT} = \sigma \ln(\sigma N_g(\sum_{z=1}^{M} G_g(z,N_g))^{-1}) + \frac{\theta_f}{N_f} \ln \phi_f^b + \theta_s \ln(1-\phi_f^b) - \sum_{z=1}^{M} \frac{u(z)}{kT} \quad (1)$$

Here θ_f and θ_s are the amount of free polymer and the amount of solvent molecules in the system, respectively, expressed in equivalent monolayers. The quantity $G_g(z,N_g)$ is the average weight of all conformations of a grafted chain of which the end segment is in layer z, and $u(z)$ is the potential energy profile of the polymer segments. When describing the interaction between two layers, it is convenient to define the excess surface free energy A^s as

$$\frac{A^s(M)}{L} = \frac{A(M)}{L} - (\mu_s - \mu_s^*)\theta_s - (\mu_f - \mu_f^*)\frac{\theta_f}{N_f} \quad (2)$$

Here, $\mu_s - \mu_s^*$ and $\mu_f - \mu_f^*$ are the chemical potentials of the solvent and free polymer, respectively, defined with respect to their pure amorphous phases (denoted by an asterisk). They are equal to:[6]

$$\frac{\mu_s - \mu_s^*}{kT} = \ln(1-\phi_f^b) + \phi_f^b(1-1/N_f)$$

$$\frac{\mu_f - \mu_f^*}{kT} = \ln \phi_f^b + (1-N_f)(1-\phi_f^b) \quad (3)$$

The interaction free energy $A^{int}(M)$ between two layers can now be written as the difference between the excess surface free energy at the given plate separation M and the excess surface free energy at infinite plate separation:

$$A^{int}(M) = A^s(M) - A^s(\infty) \quad (4)$$

Analytical Theory for a Polymer Brush Immersed in a Solution of Free Polymer. In this section we briefly review the results of Zhulina *et al.*,[7] who made an elaborate SCF analysis of polymer brushes immersed in a solution of mobile polymer. Assuming that $N_f \ll N_g$, so that the size of a mobile chain is much smaller than the characteristic length over which the volume fraction profile of the grafted chains decays, one can write the free energy density functional of mixing grafted polymer, free polymer, and solvent as:

$$l^{-3}f(z) = (1-\phi_f(z)-\phi_g(z)) \ln(1-\phi_f(z)-\phi_g(z)) + \frac{\phi_f(z)}{N_f} \ln \phi_f(z) \quad (5)$$

In the bulk solution ($z > H$, where H is the brush thickness) $\phi_g(z) = 0$, so that one can write

$$l^{-3}f^b = (1-\phi_f^b) \ln(1-\phi_f^b) + \frac{\phi_f^b}{N_f} \ln \phi_f^b \quad (5a)$$

Throughout this paper we assume the bulk solution to be infinitely large.

By combining $f(z)$ with the elastic term in the free energy of the polymer brush, one can derive an expression for the total free energy of the brush (see ref 7 for details). One can also derive equations for the grafted and free polymer volume fraction profiles ϕ_g and ϕ_f. In the next section we will discuss the interaction between two polymer brushes, which can be analyzed by studying how their free energy changes upon compression. First we discuss the shape of an isolated brush immersed in a solution of free polymer.

The volume fraction profiles of the grafted and free chains are given by the equations:[7]

$$\phi_g(z) = (1-\phi_f^b)[1-\exp\{-K^2(H^2-z^2)\}] + \phi_f^b[1-\exp\{-K^2(H^2-z^2)N_f\}] \quad (6)$$

$$\phi_f(z) = \phi_f^b \exp\{-K^2(H^2-z^2)N_f\}$$

where z is the distance from the surface and K is given by

$$K^2 = 3\pi^2/8l^2N_g^2$$

The layer thickness H can be obtained from the normalization condition

$$\int_0^H \phi_g(z)\,dz = \sigma N_g l^3$$

to give the equation

$$KH = N_g\sigma Kl + (1-\phi_f^b)D(KH) + \phi_f^b N_f^{-1/2} D(KN_f^{1/2}H) \quad (7)$$

where

$$D(x) = e^{-x^2}\int_0^x e^{t^2}\,dt$$

is the Dawson integral. Equations 6 and 7 give the volume fraction profiles ϕ_g and ϕ_f and the brush thickness H as functions of N_g, N_f, and σ. However, these equations are only valid provided $N_f \ll N_g$ and under the condition that the grafted chains are strongly stretched ($H \gg N_g^{1/2}$).

In order to extend our consideration to low grafting densities and arbitrary lengths of the free polymer chains, we have to use scaling arguments.[8] Although scaling arguments do not provide structural details of the system (volume fraction profiles, distribution of free ends, etc.), the combination of scaling and SCF results gives a general picture of a brush immersed in a polymer solution. Below, we analyze the power-law dependencies of the brush thickness and we also consider the degree of penetration of the free polymer into the polymer brush. These characteristics are studied as functions of N_f and σ. Of course, for $N_f \ll N_g$ and $H \gg N_g^{1/2}$, the explicit expressions for H, $\phi_g(z)$, and $\phi_f(z)$ are available.

Figure 1A presents a diagram of the state of a polymer brush immersed in a solution of free polymer. This figure shows the different power laws that exist for the dependence of H on σ and N_f. The boundaries between the regimes where these laws are valid are also indicated.

For high grafting densities as well as for low degrees of polymerization of the free polymer we are in region 1, which may be called the regime of "brush dominance".[8] The brush thickness scales exactly the same as in a pure low molecular weight solvent:

$$H \sim N_g\sigma^{1/3} \quad (8)$$

Regions 2 and 3 may be called the regimes of "solution dominance". In region 2 the free polymer is excluded from the brush, which is compressed by the osmotic pressure of the surrounding solution, leading to the following scaling behavior of the brush height:

$$H \sim N_g\sigma/\phi_f^b \quad (9)$$

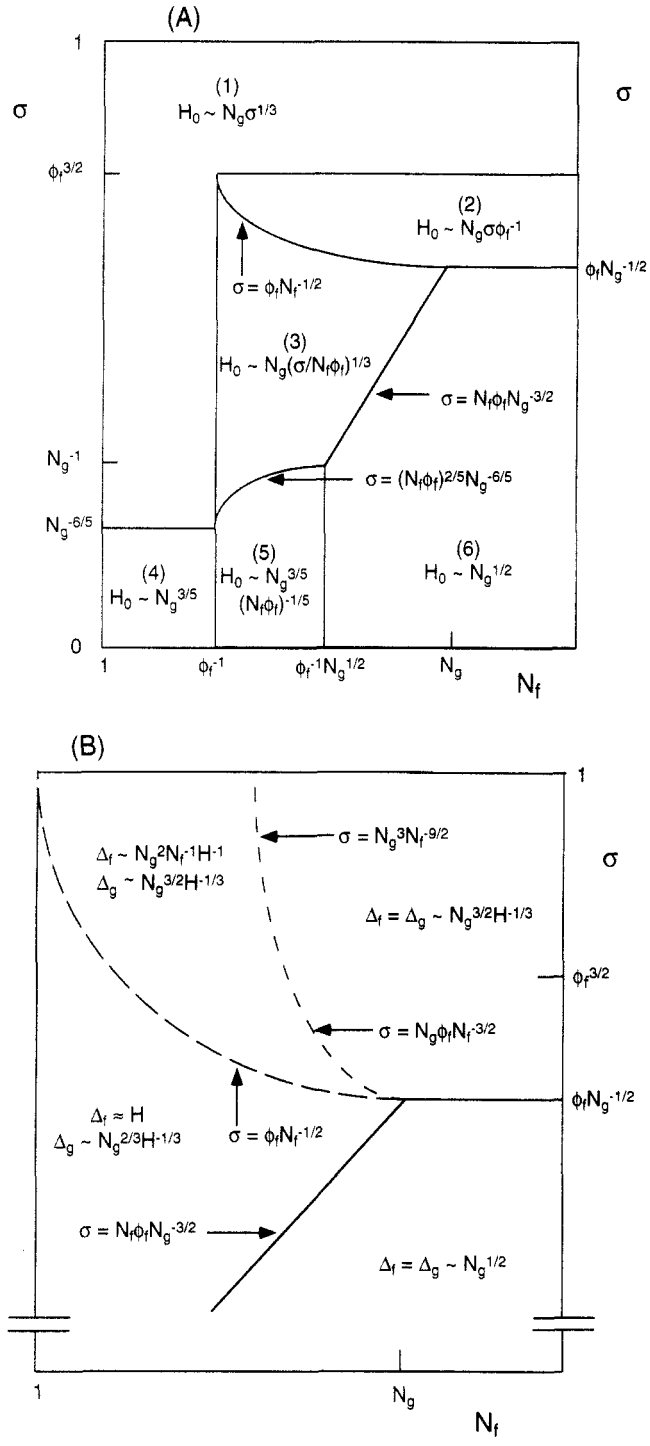

Figure 1. Diagram of the state showing the various regimes for a single grafted polymer layer immersed in a polymeric solution. The grafted polymer has a chain length N_g and is grafted at a density σ. The free polymer is chemically identical to the grafted polymer and has a chain length N_f, and its volume fraction in the bulk is ϕ_f (in the text this quantity is indicated as ϕ_f^b). In A the regions with different scaling laws for the thickness H of the grafted layer are shown. In B the boundaries are given between regions with different scaling laws for Δ_f (the penetration length of free polymer penetrating into the grafted layer) and Δ_g (the penetration length of grafted polymer penetrating into the bulk solution).

In region 3 free polymer penetrates into the brush and screens interactions between grafted polymer segments. This screening can be described by introducing an effective virial coefficient for pair interactions between these segments, $v_{eff} = (N_f\phi_f^b)^{-1} < 1$, so that the brush thickness scales as

$$H \sim V_{eff}^{1/3}N_g\sigma^{1/3} = N_g\sigma^{1/3}(N_f\phi_f^b)^{-1/3} \tag{10}$$

Equations 8–10 can be derived by expanding the expression for H given in eq 7. In regions 4–6 the grafting density is so low that the grafted chains are either nonoverlapping or only slightly overlapping (for $\sigma > N_g^{-1}$ in region 6). For small values of N_f (region 4, where $N_f\phi_f^b < 1$) the free polymer has a negligible effect and the grafted chains essentially behave as isolated coils:

$$H \sim N_g^{3/5} \tag{11}$$

For larger values of N_f ($N_f\phi_f^b > 1$) the effect of the free polymer chains can again be accounted for by introducing an effective virial coefficient, $v_{eff} = (N_f\phi_f^b)^{-1}$, so that

$$H \sim v_{eff}^{1/5}N_g^{3/5} = N_g^{3/5}(N_f\phi_f^b)^{-1/5} \tag{12}$$

For $N_f > N_g^{1/2}/\phi_f^b$ (region 6) the grafted chains can be described as Gaussian coils:

$$H \sim N_g^{1/2} \tag{13}$$

It is interesting to note that for grafting densities $N_g^{-1} < \sigma < \phi_f^b N_g^{-1/2}$ addition of free polymer to a polymer brush immersed in pure solvent can change the scaling dependence of the brush height from that of a strongly stretched polymer ($H \sim N_g$) to that of a Gaussian coil ($H \sim N_g^{1/2}$). The boundaries of the regions shown in Figure 1A can be directly found by equating the scaling dependencies on both sides of these boundaries.

Up to now we have only considered the overall brush height. A further important parameter is the degree to which the free and grafted layers interpenetrate. Let Δ_f be the penetration length of the free polymer into the brush and Δ_g the penetration length of the grafted polymer into the solution. A more precise definition of these quantities will be given in the Results section. It has previously been shown[9,10] that, for grafted polymer chains that are strongly stretched, the latter interpenetration length scales as

$$\Delta_g \sim N_g^{2/3}H^{-1/3} \tag{14}$$

This scaling relationship has a wide applicability. It is valid both for compressed and noncompressed brushes, for good and bad solvents, and for brushes immersed in a melt. One expects this scaling law to describe the degree of penetration Δ_g of the grafted chains into the polymer solution in all three regions of Figure 1A (regions 1–3) where the grafted chains are strongly stretched. The behavior of the free polymer chains is more complicated. When N_f is large, only a fraction of the segments of a free chain penetrate into the brush. These segments experience the parabolic potential profile $u(z)$ of the brush,

$$u(z) = K^2(H^2 - z^2) \tag{15}$$

with K defined below eq 6. If n segments of the free polymer chain penetrate into the brush up to a distance Δ_f from the outer boundary of the brush, then the free energy increases with an amount:

$$\frac{\Delta F}{kT} \cong \int_{H-\Delta_f}^{H} u(z)\left(\frac{dn}{dz}\right) dz \cong \frac{n}{\Delta_f}\int_{H-\Delta_f}^{H} u(z)\,dz \cong nK^2H\Delta_f \cong \frac{H\Delta_f^3}{l^4N_g^2} \tag{16}$$

The last equality in eq 16 takes into account that the free polymer chains are not stretched, so that $\Delta_f^2 \cong nl^2$. Balancing ΔF with the thermal energy ($\sim kT$), one obtains

$$\Delta_f \sim N_g^{2/3} H^{-1/3} \tag{17}$$

This scaling dependence holds when $n \approx \Delta_f^2/l^2 < N_f$ or $H > lN_g^2 N_f^{-3/2}$. For smaller values of N_f whole molecules of the free polymer penetrate into the brush. The increase in free energy due to the presence of a free polymer in the brush at a distance z' from the grafting surface is

$$\frac{\Delta F}{kT} \cong \frac{N_f^{1/2}}{l} \int_{z'-lN}^{z'} K^2(H^2 - z^2)\, dz \cong K^2 N_f (H^2 - z'^2) \cong \frac{N_f H \Delta_f}{N_g^2} \tag{18}$$

where $\Delta_f = H - z'$ and the free chains are again assumed to be Gaussian. Balancing this expression with the thermal energy leads to another scaling law for Δ_f:

$$\Delta_f \sim N_g^2 N_f^{-1} H^{-1} \tag{19}$$

This dependence should hold for $lN_g^2 N_f^{-3/2} > H > lN_g N_f^{-1/2}$. When $H < lN_g N_f^{-1/2}$, the free polymer penetrates throughout the whole brush ($\Delta_f \approx H$).

In Figure 1B the two dashed curves give the boundaries between the areas where Δ_f follows the various caling laws derived above. To the right of the curve with the short dashes (i) Δ_f equals Δ_g and scales as $N_g^{2/3} H^{-1/3}$. For $\sigma > (\phi_f^b)^{3/2}$ (i.e., for systems in region 1 of the diagram of Figure 1A) this means that the penetration lengths scale as $N_g^{1/3}\sigma^{-1/9}$. The volume fraction profiles of the grafted and free chains are symmetrical around their intersection point. The free chains only partly penetrate into the brush. Between both dashed curves (ii) whole molecules of the free polymer penetrate into the brush, but $\Delta_f < H$. The free chains penetrate farther into the brush than the grafted chains do into the solution, so that the volume fraction profiles become asymmetrical. This asymmetry is even more pronounced left of the curve with the long dashes (iii), where the free chains penetrate throughout the whole grafted layer: $\Delta_f \approx$ H, while Δ_g is still given by eq 14. In region 6 (iv), where the grafted chains are no longer strongly stretched, $\Delta_f \approx \Delta_g \approx H \approx lN_g^{1/2}$.

Analytical Theory for the Interaction between Two Brushes. We now consider the case of two interacting brushes in a solution of mobile polymer with a bulk volume fraction ϕ_f^b. Analytical expressions for the volume fraction profiles and conformational free energy of a compressed brush were obtained earlier.[7] Here we extend the results of ref 7 in order to calculate the free energy of interaction of two brushes which are compressed against each other. We take into account the redistribution of the free polymer during the compression. As before, the interpenetration of the two opposite brushes is neglected. The interacting brushes are considered as being compressed against an impermeable surface which is situated in the middle of the two grafted layers.

The equilibrium amount of free polymer as a function of the degree of compression was given in eqs 23 and 25 of ref 7. When the two brushes just do not yet overlap (so that the interplate distance $Ml = 2H$), the amount of free polymer, $\theta_f(2H)$, in the system equals:

$$\theta_f(2H) = \frac{2\phi_f^b}{\sigma} \frac{K(KN_f^{1/2}H)}{KN_f^{1/2}} \tag{20}$$

where H is given by eq 7. When the brushes are compressed, we define a compression ratio q as $Ml/2H$, which is smaller than unity for compressed brushes. The amount of free polymer decreases when q decreases. Introducing the ratio $y = \theta_f(M)/\theta_f(2H)$, we can write the following implicit equation for the amount of free polymer:

$$y = \frac{D(x)}{D(qx)} \left(\frac{KHq - \sigma' - N_f^{1/2}\phi_f^b D(x)\, y}{(1-\phi_f^b)D(x)} \right)^N \tag{21}$$

where $D(x)$ is again the Dawson integral, the normalized grafting density σ' is defined as $\sigma' = \pi(3/8)^{1/2}\sigma$, and $x = N_f^{1/2} KMl/2$. The conformational free energy $A(M)$ of a brush compressed to a distance Ml ($<2H$) is given by eq 18 of ref 7:

$$\frac{A(M)}{LkT} = \frac{M}{2\sigma}\left\{ \frac{M^2K^2}{12} + \frac{2\theta_f(M) l^3 \sigma}{N_f M} \times \ln(\theta_f(M)\sigma(\int_0^{M/2} \exp(l^2K^2N_f x^2)\, dx)^{-1}) + \left(1 - \frac{2N_g\sigma}{M} - \frac{2\theta_f(M)\sigma}{M} \ln((M/2 - N_g\sigma)(\int_0^{M/2} \exp(l^2K^2x^2)\, dx)^{-1})\right)\right\} \tag{22}$$

The interaction free energy as defined by eqs 2 and 4 is

$$A^{int}(M) = A(M) - A(2H) + \frac{(\mu_f - \mu_f^*)}{N_f}(\theta_f(2H) - \theta_f(M)) + (\mu_s - \mu_s^*)(\theta_s(2H) - \theta_s(M)) \tag{23}$$

After some rearrangements the final result becomes

$$\frac{A^{int}(M)}{LkT} = \frac{2}{\sigma K l^2}\left\{ \frac{2}{3}(KH)^3(1-q^3) - (KH)^2\sigma'(1-q^2) + \frac{\phi_f^b D(x)}{N_f^{3/2}}[y \ln(y\phi_f^b D(x)\,(D(qx))^{-1}) - \ln \phi_f^b] + (KHq - \sigma' - y\phi_f^b D(x) N_f^{-1/2}) \ln[(KHq - \sigma' - y\phi_f^b D(x) N_f^{-1/2}) \times (D(KHq))^{-1}] - (1-\phi_f^b) D(KH) \ln(1-\phi_f^b)\right\} + \frac{2H}{\sigma l}\{(1-q)(\ln(1-\phi_f^b) + \phi_f^b(1 - 1/N_f)) + (1-y)x^{-1}D(x) \times (N_f^{-1} \ln \phi_f^b - \ln(1-\phi_f^b) + N_f^{-1} - 1)\} \tag{24}$$

This equation is only valid for relatively short mobile chains, since it does not take into account the loss in conformational free energy of the chains in the gap between the two brushes. For long mobile chains this should explicitly be taken into account.

All derivations presented in this section were made for fully flexible chains (i.e., polymer chains with a Kuhn length equal to the segment diameter). The results can straightforwardly be generalized for systems with stiffer chains, for which it is more justifiable to use SCF theory.[11] However, this will not affect the free energy and other dependencies on parameters such as chain length and grafting density.

3. Results

Grafted Chains in a Polymer Solution. All lattice model results that are presented in this section were computed using a cubic lattice. Figure 2 shows volume fraction profiles of polymer brushes that are immersed in a polymer solution, calculated both with the analytical theory (eqs 6 and 7) and the lattice model. The chain

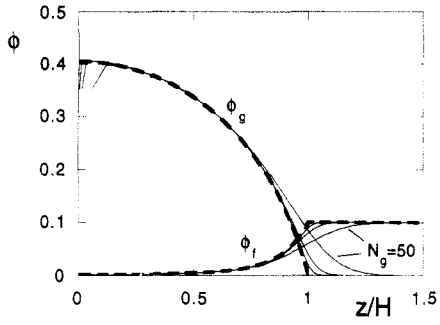

Figure 2. Volume fraction profiles of brushes immersed in a solution of short mobile polymers with chain length $N_f = 10$. The volume fractions of both grafted and free chains are given as a function of the reduced distance z/H to the grafting surface. The layer height H has been calculated using eq 7. The dashed curves give ϕ_g and ϕ_f as predicted by eq 6 (these curves do not depend upon N_g as $H \sim N_g$). The solid curves follow from lattice model calculations. Further parameters: N_g = 50, 200, and 600; σ = 0.1; ϕ_f^b = 0.1.

length N_f of the mobile polymer is 10 segments, and the lattice calculations (solid curves) have been made for grafted polymer chain lengths N_g of 50, 200, and 600. According to eq 7, $H \sim N_g$, so that the volume fraction profiles given by eq 6 (dashed curves) are independent of N_g if they are plotted as a function of the reduced distance z/H. The longer the grafted chain length, the better the agreement with the analytical equations. For shorter grafted chain lengths the profile of the grafted component shows a clear "foot" protruding into the solution. The shorter chains also show a clear depletion zone near the surface, which is absent in the analytical model. These features are completely analogous to the situation where the brush is immersed in a one-component low molecular weight solvent. The system of Figure 2 belongs to region 1 of the phase diagram of Figure 1A. The volume fraction profiles of the free and grafted chains are asymmetric around their intersection point. This is especially clear for high N_g. Whole molecules of the free component (which are only 10 segments long) move into the brush, but they do not penetrate further than approximately 50% of the brush height.

In Figure 3 the analytical model is compared with the lattice calculations for systems in regions 1 (σ = 0.1), 2 (σ = 0.02), and 3 (σ = 0.004) of the phase diagram. The bulk volume fraction of free polymer has a value of 0.1 in all cases. In each case the results are shown for a small free polymer (N_f = 30, which is 5% of the chain length of the grafted polymer) and for a larger free polymer (N_f = 300, which is half the grafted chain length). In the derivation of eq 6 it was assumed that $N_f \ll N_g$. Indeed, for all three grafting densities shown in Figure 3 the curves for N_f = 30 show better agreement between the lattice calculations and eq 6 than do the curves for N_f = 300. For N_f = 30 the brush thickness H is described well by eq 7. The penetration length Δ_g decreases with increasing H and is approximately given by eq 14. The free polymer penetrates the brush over a length Δ_f which exceeds Δ_g and becomes equal to H for low grafting densities; these trends agree well with the scaling relations given in Figure 1B.

The analytical volume fraction profiles of the grafted component deviate slightly from the lattice calculations at the surface and at the periphery of the layer. These are well-known effects that are also seen with brushes immersed in a one-component low molecular weight solvent. The presence of the surface leads to a narrow depletion layer for the grafted polymer, and because of their finite chain length, some chains stretch farther away from the surface than they should according to eq 6. For N_f = 300 eq 7 still gives a good estimate of the brush height, but it predicts a far too sharp boundary of the grafted and free polymer layers. Especially for the higher grafting densities this effect is very pronounced. It is caused by the very approximate way in which the translational entropy of the mobile chains is accounted for in the derivation of eq 6.

If a full description is wanted of the system consisting of grafted polymer immersed in a solution of relatively long free polymer chains, one must combine eq 7 with the scaling dependencies of the penetration lengths Δ_f and Δ_g. These were given in the previous section (eqs 14–19). In Figure 3 the lattice curves for N_f = 30 are asymmetric around the intersection point of the two profiles. This is in agreement with the prediction for the region left of the curve with the short dashes in Figure 1B. For N_f = 300 one moves into the symmetrical region, so that $\Delta_f = \Delta_g$. The scaling dependence of Δ_f on N_f, N_g, and H is shown in Figures 4 and 5. In all cases the penetration length has (arbitrarily) been defined as the distance over which $\phi_f(z)$ falls from $\phi_g(z)$ (i.e., the intersection point of both profiles) to half this value. The systems which correspond to the data points of Figure 4 are described in Table 1. They all belong to the symmetric area of the phase diagram. The penetration length Δ_f indeed scales as $N_g^{2/3}H^{-1/3}$, as predicted by eq 17. Table 2 gives the systems that are shown in Figure 5. These belong to the asymmetric area of the phase diagram. In this case the penetration length Δ_f scales as $N_g^2(N_fH)^{-1}$, as expected from eq 19.

Up to now we have considered grafted polymer chains that are strongly stretched ($H \sim N_g$, regions 1–3 of the phase diagram). When $\sigma < \phi_f^b N_g^{-1/2}$, an increase of the chain length of the mobile polymer leads to a transition of the grafted chains from a strongly stretched ($H \sim N_g$) to a Gaussian coil conformation ($H \sim N_g^{1/2}$). Equation 6, whose derivation was based upon the grafted chains being strongly stretched, is then no longer valid. In Figure 6 lattice calculations are shown for systems that are expected to show this Gaussian coil behavior. Only the volume fractions of the grafted component are shown. Reduced coordinates have been used to clearly demonstrate the scaling behavior of the grafted polymer chains. One can conclude from Figure 6 that H indeed scales as $N_g^{1/2}$. However, the volume fraction profiles themselves do not precisely obey this scaling relationship: the scaled profiles do not exactly collapse onto one master curve.

Interaction between Two Brushes in Pure Solvent. Figure 7 shows interaction curves for the compression of two polymer brushes in a pure solvent (no free polymer present). The solid curve is the analytical prediction of eq 24, where in this case all terms containing ϕ_f^b and y vanish. The other curves were obtained from the lattice model for N_g = 50, 200, and 600. The insets show the interaction on a semilogarithmic scale. Equation 24 predicts that $A^{int}(q) \sim N_g$. For long chains the lattice calculations approach the prediction of eq 24. The agreement also becomes better for larger grafting densities (see Figure 7B). These trends are the same as those found when comparing volume fraction profiles of noncompressed brushes. For small compressions ($q \approx 1$) relatively large deviations remain between the lattice calculations and the strong-stretching model, even for long chain lengths. This is most clearly seen from the curves drawn on a semilogarithmic scale. Here only the outermost part of the brush is being compressed. In this case the exponential decay (foot) of the profile, predicted by the lattice model, has a relatively strong effect on the

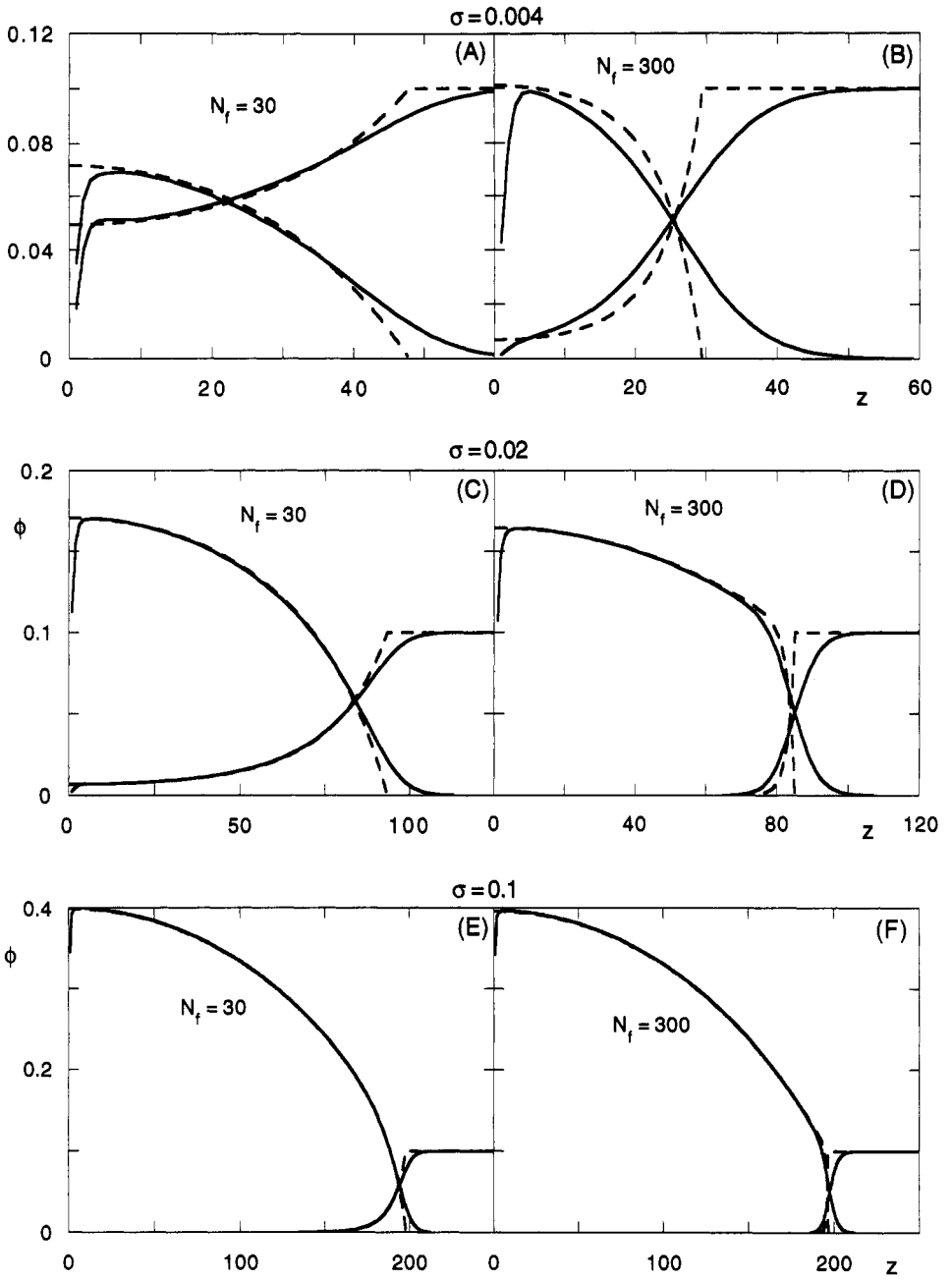

Figure 3. Volume fraction profiles of brushes immersed in solutions of relatively short ($N_f = 30$) and relatively long ($N_f = 300$) mobile polymers. The dashed curves follow from eq 5, and the solid curves are lattice calculations. In all cases $N_g = 600$ and $\phi_f^b = 0.1$. The grafting density and free chain length are indicated in the graphs.

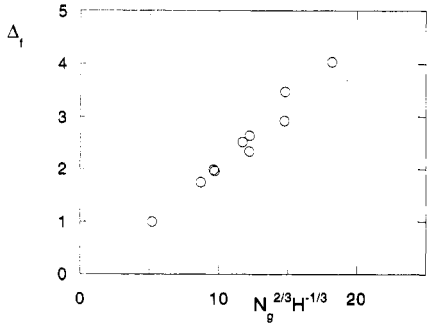

Figure 4. Penetration length Δ_f of the free polymer into the brush as a function of grafted chain length, N_g, and brush height, H. The systems presented in this figure belong to the "symmetric area" of Figure 1B. The data of these systems are given in Table 1.

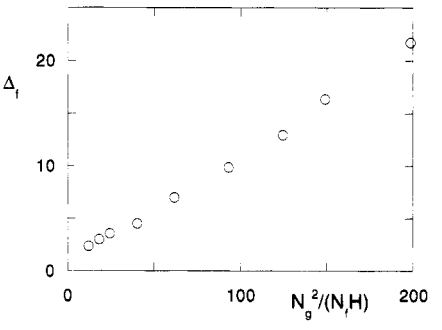

Figure 5. Same as Figure 5 for systems that are in the "asymmetric area" of Figure 1B. The data of these systems are given in Table 2.

interaction curve. This causes the interaction free energy to have a finite positive value for values of q larger than unity.

In Figure 8 volume fraction profiles calculated from the lattice model are given for $N_g = 600$ and $\sigma = 0.01$. The profiles of the brushes on both surfaces are drawn individually for three interplate distances: $M = 200$ ($q = 1.03$), $M = 50$ ($q = 0.26$), and $M = 20$ ($q = 0.10$). Note the

Table 1

N_g	σ	N_f	ϕ_f^b	$N_g^{2/3}H^{-1/3}$	Δ_f
100	0.5	200	0.1	5.2029	0.99538
300	0.1	200	0.1	8.7143	1.7501
300	0.5	200	0.5	9.7201	1.9633
300	0.1	200	0.1	9.6549	1.9923
300	0.5	200	0.5	11.713	2.5159
600	0.1	6000	0.1	12.205	2.3393
600	0.1	200	0.1	12.226	2.6399
600	0.1	600	0.5	14.758	2.9248
600	0.1	200	0.5	14.802	3.4746
600	0.01	600	0.1	18.171	4.0375

Table 2

N_g	σ	N_f	ϕ_f^b	N_g^2/N_fH	Δ_f
200	0.1	50	0.1	12.054	2.3500
200	0.1	50	0.1	18.250	2.9801
400	0.1	50	0.1	24.446	3.5590
200	0.25	10	0.1	40.374	4.4948
200	0.1	10	0.1	61.696	6.9966
300	0.1	10	0.1	93.175	9.8712
400	0.1	10	0.1	124.64	12.986
300	0.1	10	0.5	149.00	16.394
400	0.1	10	0.5	198.61	21.709

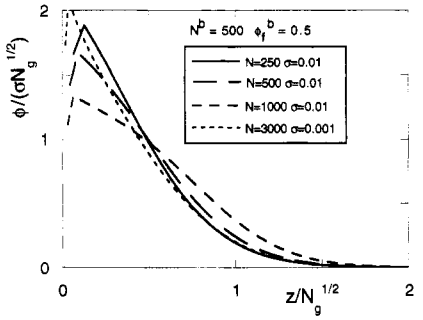

Figure 6. Volume fraction profiles of systems in region 6 of Figure 1. Only the grafted chains are shown. All curves are lattice calculations. The reduced distance to the grafting surface $zN_g^{-1/2}$ is used as the abscissa to check the relationship $H \sim N_g^{1/2}$. The reduced volume fraction $\phi/(\sigma N_g^{1/2})$ is used as the ordinate so that the areas under all curves are equal. In all cases $\phi_f^b = 0.5$ and $N_f = 500$. The values of σ and N_g are shown in the figure.

different scales for the three diagrams. In Figure 8A (q = 1.03) the brushes just start to interact with each other. Although $q > 1$, so that according to the "classical" prediction of eq 24 there should not yet be any interaction, the tips of both profiles do already slightly overlap, giving rise to a finite free energy of interaction, which is neglected in the analytical theory.

The analytical theory further neglects the fact that when two brushes are compressed against each other, the chains attached to both surfaces will to a certain extent interpenetrate. This can be clearly seen in parts B and C of Figure 8. Such interpenetration was also seen in the molecular dynamics study of Murat and Grest[12] and the recent Monte Carlo simulations of Chakrabarti, Nelson, and Toral.[13] Decreasing the plate separation eventually leads to a complete overlap of both layers. Taking into account this interpenetration should lead to a slightly less repulsive interaction.

In Figure 9 the effect of this interpenetration on the free energy of interaction is quantified for a brush with a chain length of 200 segments and a grafting density of 0.01. The results of the lattice model are given for three different cases. The first is the compression of two brushes on opposite surfaces (which is denoted in the figure legend as "two brushes"). This is exactly the same system as shown in the previous figures. In the second case a single

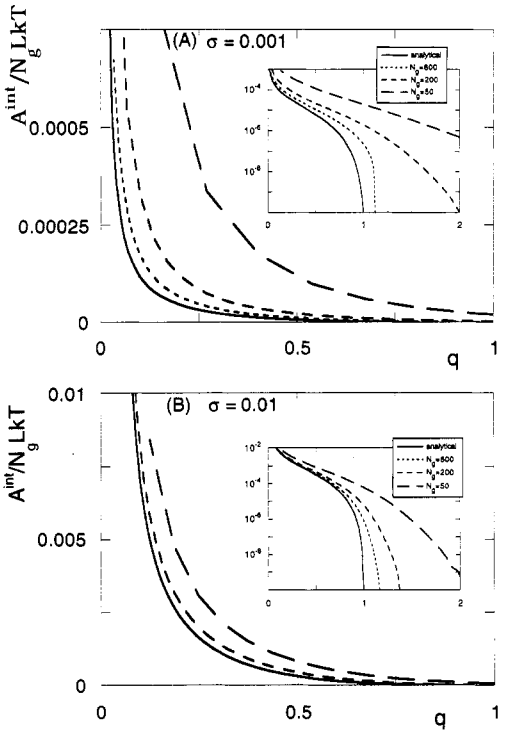

Figure 7. Interaction curves between two brushes in the absence of free polymer. The lattice calculations for N_g = 600, 200, and 50 are compared with eq 24 (solid curve). Grafting density: σ = 0.001 (A); 0.01 (B). The insets show the interaction free energies on a semilogarithmic scale.

brush (denoted as "one brush") is compressed by a bare surface (i.e., a surface bearing no grafted polymer); q is now defined as Ml/H. In this case there is no interpenetration, as the chains cannot move through the surface by which they are compressed. Therefore, one would expect a better agreement with eq 24. However, the agreement is worse. Below we explain the reason for this discrepancy. The curves denoted by "adsorbing chains" in Figure 9 have been calculated for the same system as that denoted by one brush, but now the segments of the polymer have a small attractive interaction with the bare surface. The value of this attraction can be described by the adsorption energy χ_s as defined by Silberberg.[14] We have chosen $\chi_s = -\ln(5/6)$, which is the critical adsorption energy of an infinitely long polymer chain on a cubic lattice.

For all three cases of Figure 9 the lattice calculations give a more repulsive interaction than that predicted by the analytical theory. At any separation the compression of a brush by a bare surface is more repulsive than the similar compression by another brush. The difference between these two systems is not, however, solely due to the interpenetration that occurs between the two brushes. The bare surface also imposes entropical restrictions on the conformations of the grafted polymer chains. This unfavorable entropical interaction is compensated when there is an attractive interaction of the segments with the surface, as is the case for the curves denoted by adsorbing chains. The adsorbing chain curve and the curve for two brushes virtually coincide, except for very small compressions ($q > 1$). When the outermost parts of two brushes start to overlap, the interpenetration of the chains leads to a decrease in the repulsive interaction. For $q < 1$ this effect has become negligible.

At high compressions the two layers very strongly overlap. Nevertheless, for small values of q the analytical equations for the free energy of interaction (where this overlap is neglected) agree very well with the lattice

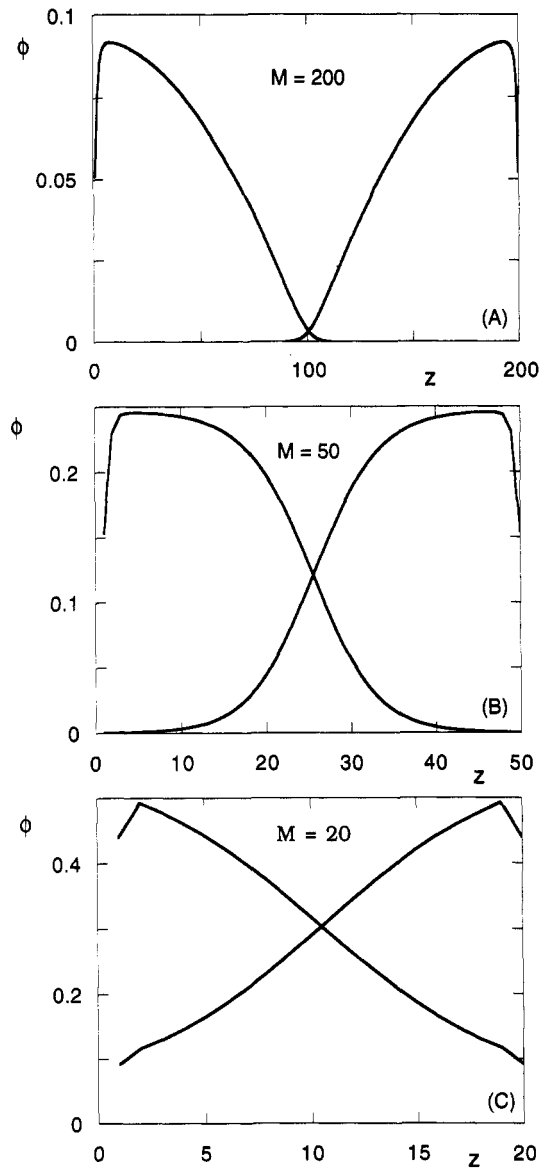

Figure 8. Volume fraction profiles of two brushes that are compressed against each other. $N_g = 600$; $\sigma = 0.01$. The degrees of overlap are as follows: for $M = 200$, $q = 1.03$; for $M = 50$, $q = 0.26$; for $M = 20$, $q = 0.10$.

calculations. In this region the osmotic pressure forms the major contribution to the free energy, so that the exact shape of the volume fraction profile becomes less important.

In Figure 10 the amount of interpenetration is plotted for six different systems. The interpenetration length Δ has been defined as the distance from the midplane to the plane where the penetrating chains have a volume fraction equal to half their volume fraction in the middle. The parameter Δ is expected to scale as $N_g^{2/3}M^{-1/3}$,[4] analogous to the scaling relation given in eq 14 for the interpenetration distance Δ_g of a brush into a polymer solution. We may indeed conclude from Figure 10 that $\Delta \sim N_g^{2/3}M^{-1/3}$, irrespective of chain length, grafting density, and solvency ($\chi = 0$, good solvent; $\chi = 0.5$, Θ solvent). For small values of M the data of all six systems obey this scaling relationship rather accurately. Of course, it is to be expected that for larger values of M deviations occur. In these cases the calculated points do not lie on the master curve. When M becomes twice the brush height, there cannot be any interpenetration at all.

Interaction between Two Brushes Immersed in a Polymer Solution. Figure 11 shows interaction curves

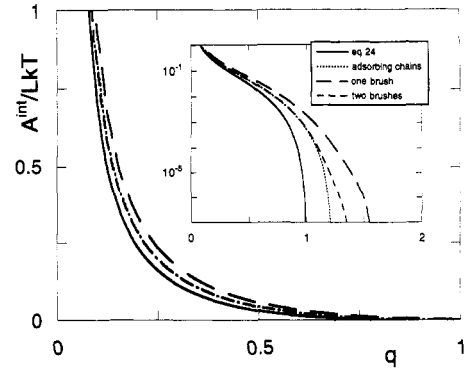

Figure 9. Interaction curves between two brushes and between a brush and a wall. Parameters: $N_g = 200$; $\sigma = 0.01$. The solid curve is calculated using eq 24. The curve "two brushes" is the free energy of interaction when two similar brushes are compressed against each other; in this case the chains in both brushes can interpenetrate. The "one brush" curve gives the free energy of interaction of a single brush which is compressed by a hard impenetrable surface. The "adsorbing chains" curve is calculated for the same system, but in this case the grafted polymer chains have a small adsorption energy for the surface which compresses them.

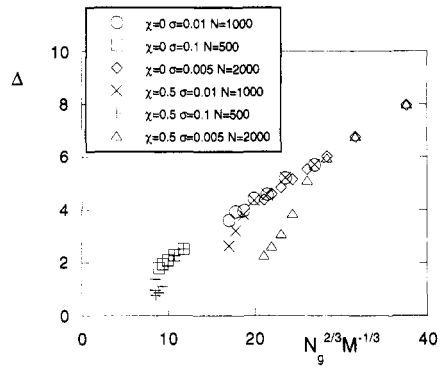

Figure 10. Distance of interpenetration, Δ, when two equal brushes are compressed against each other. M is the distance between both grafting surfaces, expressed in number of lattice layers. This figure checks the scaling dependence predicted by eq 14.

of brushes in a polymer solution. An important parameter in the calculation of $A^{int}(q)$ is the amount of mobile polymer, $\theta_f(M)$, between the plates when they are at an arbitrary separation M. Figure 12 shows the relative amount of free polymer in the system, $y = \theta_f(q)/\theta_f(q=1)$, for $N_g = 600$, $\sigma = 0.01$, and $N_f = 10$ and 50. There is excellent agreement between the lattice model and the prediction of eq 21 for the amount of free polymer expelled from the gap between the brushes.

In all cases of Figure 11, for large compressions ($q < 0.5$) the analytical equations agree very well with the lattice calculations. The inset for $N_f = 10$ shows the interaction curve on a linear scale. Plotted on this scale the figure shows that over the whole range of q eq 24 predicts the interaction very well when free polymer chains are present in the system. For the other values of N_f (50, 200, and 600) a linear plot (not shown) displays the same agreement between the two models. To study the interaction at $q \approx 1$, it is more convenient to plot the free energy of interaction on a logarithmic scale, as is done in Figure 11 for all four values of N_f. The lattice calculations predict a more repulsive interaction for small compressions, which is due to the foot in the volume fraction profile. This is similar to the case for a polymer brush in a pure solvent. The contribution of the foot turns out to depend on the free chain length. For $N_f = 50$ or 200 it shows up for slightly larger values of q than it does for $N_f = 10$, but for $N_f =$

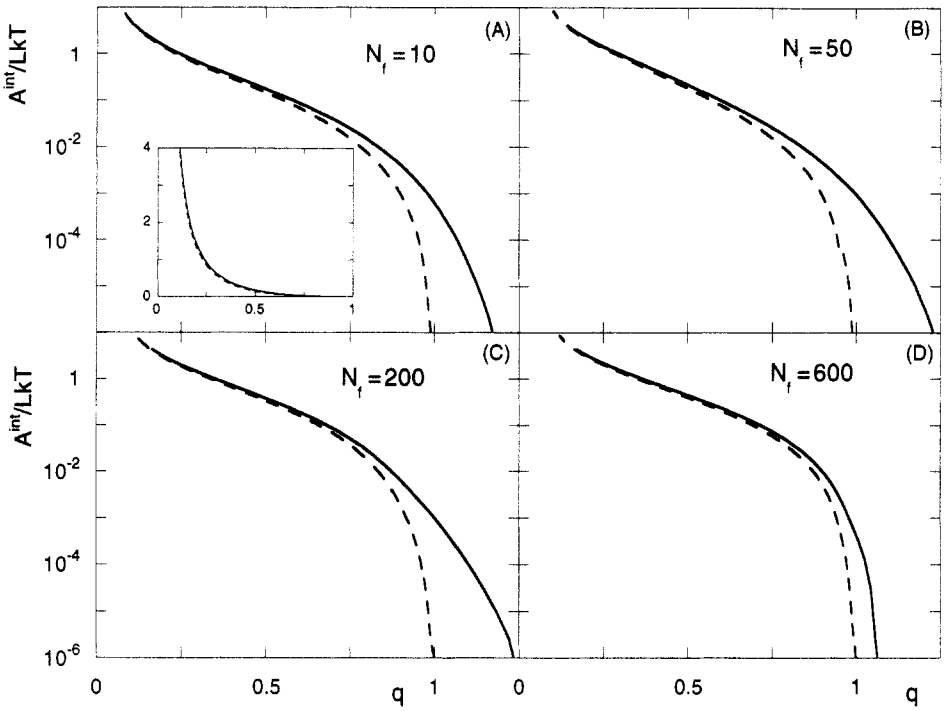

Figure 11. Interaction curves of two brushes in a polymer solution for various chain lengths of free polymer: N_f = 10 (A), 50 (B), 200 (C), and 600 (D). Other parameters: N_g = 600; σ = 0.01; ϕ_f^b = 0.1. The inset shows the data for N_f = 10 on a linear scale. All other graphs are on a semilogarithmic scale.

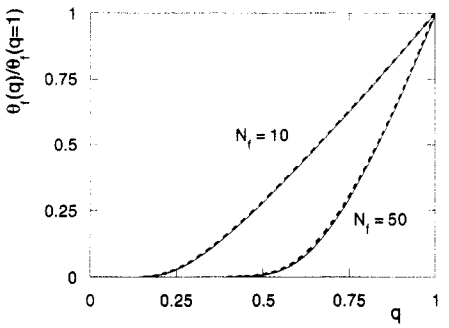

Figure 12. Fraction of free polymer remaining between two brushes when these are compressed for two values of N_f. Other parameters: N_g = 600; σ = 0.01; ϕ_f^b = 0.1.

600 the contribution of the foot seems to become less important.

However, for high N_f the situation is more complicated, as is shown in Figure 13. Increasing the chain length of the mobile polymer leads to an attractive minimum in the interaction curve for $q > 1$. For $N_f = 600$ (=N_g) this starts to have an important effect on the total interaction free energy for small compressions. Van Lent *et al.*[15] extensively studied this attraction between polymer brushes in a polymeric solution. It is an effect that has also been found experimentally and can be easily understood for the limiting case when there is no grafted polymer (i.e., $\sigma = 0$). Due to the depletion of free polymer in the vicinity of the surfaces, an attractive osmotic force appears. Some experimental results indicate that this attraction can also exist when the surfaces are covered by a grafted layer (see, for example, ref 16 and the references given therein). Van Lent *et al.* showed that such an attraction is predicted by the SCF lattice theory. However, they only considered systems for which $N_f \geq N_g$. For all values of ϕ_f^b an increase of N_f then leads to a deeper attractive minimum in the interaction curve. In contrast with the situation that no grafted polymer is present, this attraction was shown to be an entropic effect caused by the grafted chains themselves and not directly by the free polymer. The

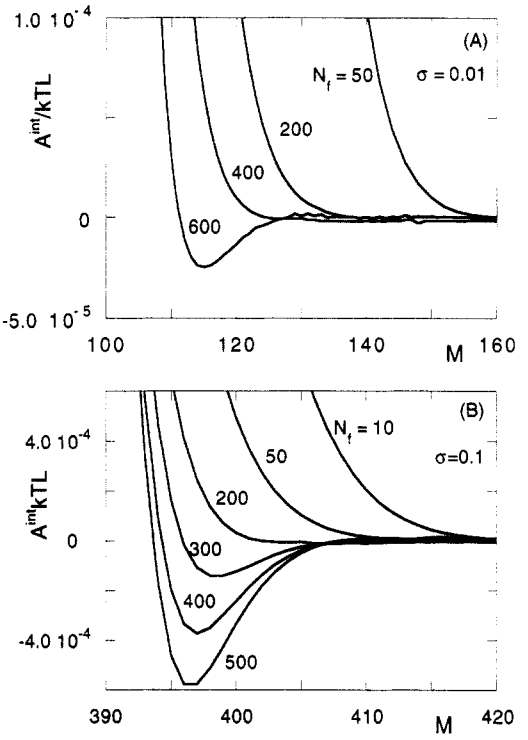

Figure 13. Effect of the chain length of the mobile polymer on the interaction curves near the onset of interaction (q around 1). For large values of N_f an attractive minimum appears. In part A, σ = 0.01, and in part B, σ = 0.1. Other parameters: N_g = 600; ϕ_f^b = 0.1.

grafted chains mix more easily with chains from the other grafted layer than with the free polymer coils.

Figure 13 shows that in order to find an attractive minimum the free polymer must exceed a certain minimum chain length. Increasing the grafting density decreases this minimum value of N_f. For example, when N_f = 400, there is no attractive minimum if σ = 0.01 (Figure 13A), but for the higher grafting density σ = 0.1, such a minimum does occur (Figure 13B). In Figure 13 for any q the

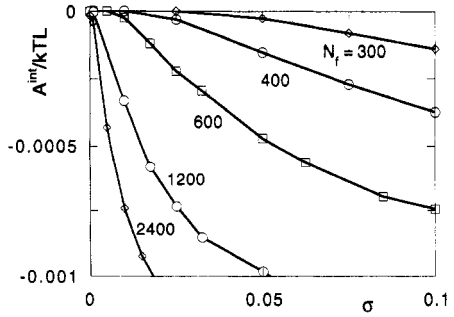

Figure 14. Depth of the minimum in the interaction curve as a function of grafting density. Parameters: $N_g = 600$; $\phi_f^b = 0.1$. The values of N_f are indicated in the figure.

repulsion is larger for shorter N_f. Furthermore, the minimum shifts to a smaller plate separation when N_f is increased. In Figure 11 this trend was not found for the dependency of the repulsion on N_f. This can be explained by the fact that in Figure 11 the free energy of interaction is given as a function of the relative compression q, whereas in Figure 13 it is given as a function of the plate separation M. The brush height itself depends on N_f, which explains the apparent nonmonotonic dependency of the repulsion on N_f found in Figure 11.

It would be useful to interpret these results using the diagram of state of Figure 1. We find that attraction only occurs for strongly stretched chains, when the grafted and free polymer profiles are symmetric around their intersection point (region 1 for high N_f). However, this symmetry condition is not sufficient for attraction to occur. If it were, then in Figure 13 there should be an attraction for $N_f > N_g^{2/3}\sigma^{-2/9}$ when $\sigma > (\phi_f^b)^{3/2}$ (i.e., $N_f > 119$ when $\sigma = 0.1$). The minimum value of N_f turns out to be larger than this. For a system in which there is an attractive minimum, the depth of this minimum depends on the grafting density. This is shown in Figure 14, where the value of the attractive minimum is given as a function of σ. This is done for a constant grafted chain length ($N_g = 600$) and five different free chain lengths. For small N_f the attraction disappears completely below a certain grafting density. Only at extremely low densities does it then reappear again. This is difficult to see in the figure because the curves practically coincide with the left ordinate axis. That the attraction must reappear at low coverages is obvious; as for $\sigma = 0$ one recovers the depletion attraction of two surfaces without grafted layers. However, Figure 14 shows that increasing the grafting density from zero to just a very low value ($\sigma < N_g^{-1}$) already makes the attraction disappear. The grafted chains then still have unstretched conformations. This corresponds with the bottom part of Figure 1A.

4. Discussion and Conclusions

In this paper we have explored the applicability of the strong chain stretching approach to give an SCF description of end-grafted polymer layers that interact either with each other or with free polymer in solution. This approach has previously been shown to agree very well with more exact lattice calculations in describing isolated (i.e., noninteracting) grafted layers. In this case significant deviations occur only very close to the surface (depletion effect) and at the periphery of the grafted layer (exponential decay of the volume fraction profile). For long enough polymer chains these deviations are negligible, but for short chain lengths they may become important.

Our lattice calculations indeed show that the onset of interaction between two brushes is situated at a larger distance than twice the "strong-stretching brush height" (for which we defined the reduced surface separation q to be unity). For $N_g = 50$ and $\sigma = 0.01$, representative of the adsorption of a short block copolymer, there is already a free energy of interaction on the order of $10^{-3}\,kT$ per lattice site for $q = 1.25$. Assuming a lattice spacing l on the order of 1 nm, this is an interaction that should be just within the detection limit of the surface force apparatus. In this context it is interesting to note that Milner[17] made a quantitative comparison between experimental force–distance data and strong chain stretching SCF equations. Only at large separations did he find the theoretical repulsion to be significantly lower than the experimental data. Although he prefers to explain this discrepancy by a polydispersity argument, our calculations suggest that it may also be explained by the approximate character of the strong-stretching theory and would even occur for completely monodisperse brushes. In Figure 7 one can also see that even for long chain lengths ($N_g = 600$) and large compressions ($q < 0.25$) there is still a small difference between the lattice calculations and eq 24. This may be caused by the depletion zone next to the surface, which is still present for small values of M (see Figure 8).

When two polymer brushes are compressed against each other, the distance Δ over which chains penetrate into the opposite layer scales as $N_g^{2/3}M^{-1/3}$ (Figure 10). This interdigitation has, however, hardly any effect on the normal force between both layers. But that does not necessarily mean that the overlap of both grafted layers is of no consequence whatsoever. When the polymer brushes are compressed and subsequently a lateral (shearing) force is applied, the overlap of both layers will probably significantly influence the interaction. In principle, this can be investigated using the apparatus of Klein *et al.*,[18] which measures both normal and lateral forces.

When polymer is added to the solution in which a polymer brush is immersed, the grafted layer is compressed. The resulting volume fraction profiles of the grafted and free components are given by eq 6. For short free chain lengths this equation gives as good a description of the profiles as the strong-stretching theory does for brushes immersed in a one-component low molecular weight solvent. For longer free chain lengths the overlap area of the grafted and free components is described poorly. However, as far as only the brush height is concerned, eq 7 still agrees very well with the lattice calculations.

A new feature we have added to the system of grafted plus free polymer is the penetration lengths of both components into the opposite phase. Using simple thermodynamic arguments, we derived scaling laws for the two penetration lengths in different parts of the diagram of states. These scaling laws were corroborated by the lattice calculations. In principle, it is possible to determine the volume fraction profiles of the grafted and free chains individually in a neutron reflectivity experiment. By contrast-matching one of the two components with the solvent, only the other component is detected. Thus the interpenetration of both layers might be checked experimentally. As far as we know this has not yet been done.

When free polymer is present in the solution, eq 24 can be used for the free energy of interaction between two brushes (this equation predicts a purely repulsive interaction). Only when the free polymer chain length exceeds a critical value (which depends upon the grafting density and grafted polymer chain length) does the interaction profile which is obtained from the lattice model acquire a qualitatively new feature: for $q \geq 1$ an attractive minimum appears. It is not possible to explain this in

terms of the diagram of state in Figure 1. The minimum is deepest when $\sigma = 0$ (i.e., for hard surfaces). For relatively short chain lengths ($N_f < N_g$) even a very small amount of grafted polymer already causes the attraction to disappear. It should be possible to verify this prediction experimentally. Practical applications are perhaps possible in systems where depletion attraction undesirably leads to flocculation.

Acknowledgment. We are grateful to Dr. Frans Leermakers for helpful discussions. E.B.Z. was supported by The Netherlands Foundation for Chemical Research (SON) with financial aid from The Netherlands Organization for Scientific Research (NWO).

References and Notes

(1) Wijmans, C. M.; Scheutjens, J. M. H. M.; Zhulina, E. B. *Macromolecules* **1992**, *25*, 2657.
(2) Semenov, A. N. *Sov. Phys. JETP* **1985**, *61*, 733.
(3) Milner, S. T.; Witten, T. A.; Cates, M. E. *Macromolecules* **1988**, *21*, 2610.
(4) Zhulina, E. B.; Borisov, O. V.; Priamitsyn, V. A. *J. Colloid Interface Sci.* **1990**, *137*, 495.
(5) Evers, O. A.; Scheutjens, J. M. H. M.; Fleer, G. J. *Macromolecules* **1991**, *24*, 5558.
(6) Flory, P. J. *Principles of Polymer Chemistry*; Cornell University Press: Ithaca, NY, 1953.
(7) Zhulina, E. B.; Borisov, O. V.; Brombacher, L. *Macromolecules* **1991**, *24*, 4679.
(8) de Gennes, P.-G. *Macromolecules* **1980**, *13*, 1069.
(9) Zhulina, E. B.; Semenov, A. N. *Polym. Sci. USSR* **1989**, *31*, 196.
(10) Witten, T. A.; Leibler, L.; Pincus, P. A. *Macromolecules* **1990**, *23*, 824.
(11) Fleer, G. J.; Cohen Stuart, M. A.; Scheutjens, J. M. H. M.; Cosgrove, B.; Vincent, B. *Polymers at Interfaces*; Chapman & Hall: London, 1993.
(12) Murat, M.; Grest, G. S. *Phys. Rev. Lett.* **1989**, *63*, 1074.
(13) Chakrabarti, A.; Nelson, P.; Toral, R. *J. Chem. Phys.* **1994**, *100*, 748.
(14) Silberberg, A. *J. Chem. Phys.* **1968**, *48*, 2835.
(15) Van Lent, B.; Israels, R.; Scheutjens, J. M. H. M.; Fleer, G. J. *J. Colloid Interface Sci.* **1990**, *137*, 380.
(16) Vincent, B.; Edwards, J.; Emmet, S.; Jones, A. *Colloids Surf.* **1986**, *18*, 261.
(17) Milner, S. T. *Europhys. Lett.* **1988**, *7*, 695.
(18) Klein, J.; Perahia, D.; Warburg, S. *Nature* **1991**, *352*, 143.